# Numerical study of the microstructure in ferromagnetic shape memory alloys

Jonathan F. Gebbia
*Facultat de Física, Universitat de Barcelona, Diagonal 645, 08028 Barcelona, Spain.**

**Abstract:** The microstructural behavior of ferromagnetic shape memory alloys (FSMAs) is studied by means of simulations of a magnetoelastic model. The elastic part consists of a Ginzburg-Landau free energy, extended to include both long-range anisotropic interactions and disorder, whereas the magnetism is based on the micromagnetic theory. The model is able to reproduce several experimental microstructures. First, the pure elastic model is tested and the structural martensitic transformation, the shape memory effect (SME) and the superelastic effect are found. Simulations of the full magnetoelastic model show, at temperatures $T < T_c$, magnetic stripes within martensitic twins. The martensitic transformation and the evolution of the magnetization with $T$ is observed by different values of applied magnetic field. Also, the magnetic shape memory effect is obtained and the evolution of microstructure is presented in the magnetic field-temperature-strain curve. The parameters used in these simulations are experimental values corresponding to Fe-Pd FSMA.

## I. INTRODUCTION

Ferromagnetic materials are the most paradigmatic among *ferroic* materials. Ferroic materials are characterized by the existence of a phase transition from a high-symmetry (disordered) phase towards a low-symmetry (ordered) phase when lowering the temperature ($T$) [1]. This transformation can be characterized by an order parameter (OP) that vanishes above the transition temperature and takes non-zero values below it. Particularly, the ferromagnetic systems exhibit a spontaneous net magnetization below the Curie Temperature. Other examples of ferroics are ferroelectrics and ferroelastics, where the OPs are respectively the polarization and the strain. All of them, show in the ordered phase a multidomain mesostructure due to, among other causes, the presence of long-range interactions. The phase transition can also be induced by the application of the external field and presents hysteresis behavior.

Materials that show multiple ferroic behaviors are called *multiferroics*. These materials present a coupling among two (or more) ferroic properties and they exhibit a relevant cross-variable response by the application of a non-conjugate external field (Fig. 1) [2]. For example, a multiferroic that presents ferromagnetism and ferroelectricity at the same time has a magnetoelectric coupling so that an electric field can affect the magnetization as well as the magnetic field affects the polarization. The effect of cross-variable responses opens a wide range of technological applications.

The study presented in this report is focused in ferromagnetic shape memory alloys (FSMAs). These materials exhibit a structural transition in the ferromagnetic phase, specifically a first-order displacive transformation, where the low-symmetry phase is usually called *martensite* and the high-symmetry one *austenite*.

These alloys show a magnetoelastic coupling and therefore they have a cross-response of strain-magnetic field and magnetization-stress field. This gives rise to various interesting effects such as shape memory effect and superelasticity both induced by external magnetic field, hysteresis loop in strain-magnetic field and magnetization-stress field curves, etc. [4]-[5]

| Order Parameter | Conjugate Field |
|---|---|
| Magnetization, **M** | Magnetic, **H** |
| Polarization, **P** | Electric, **E** |
| Strain, $\epsilon$ | Stress, $\sigma$ |

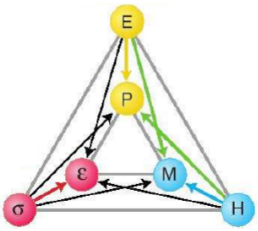


FIG. 1. The table (left) shows order parameters associated to some ferroic systems and their respective conjugate fields. The diagram (right) shows the coupling between different magnitudes giving rise to a cross-variable response in multiferroics. Extracted from Ref [3].

The goal of this study is to reproduce the above mentioned effects by means of numerical simulations of a 2D system using a Ginzburg-Landau model for the description of *square-to-rectangular* martensitic transformation (MT) that also includes contributions due to disorder and anisotropic long-range interations, and micromagnetic model for the description of magnetics interactions. Also, the model takes into account a term for magnetoelastic coupling which is the term that will allow us to reproduce cross responses between elasticity and magnetism.

## II. MODEL:

### A. Elastic Model

The description of the MT is given by the Ginzburg-Landau theory [6]. According to elasticity theory, any deformation undergone by a system with square symmetry can be described as a superposition of three symmetry-

* jgebbimo8@alumnes.ub.edu

adapted strains [7]: compressive $e_1$, deviatoric $e_2$ and shear $e_3$ strains (see Fig. 2). As it can be seen, the appropiate Landau OP for the square-to-rectangular transition is the deviatoric strain $e_2$.

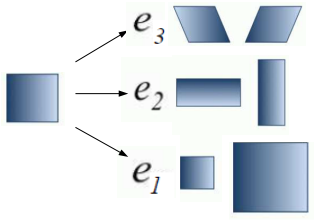


FIG. 2. Symmetry adapted strains: $e_1$, $e_2$ and $e_3$ stand for the bulk, deviatoric and shear strains. Extracted from Ref [3]

The twofold degeneracy of the low temperature phase requires that $f_L(e_2) = f_L(-e_2)$ in the Landau expansion. On the other hand, a system undergoing a MT typically achieves a multivariant structure, with the presence of domain boundaries. Ginzburg proposed an extra energetic penalty for variations of the OP, $f_{\rm G} = \frac{\kappa}{2}|\nabla e_2|^2$. Therefore, the Ginzburg-Landau free energy density is $f_{\rm L,G} = f_L + f_{\rm G}$:

$$f_{\rm L,G}[e_2] = \frac{A_2}{2}e_2^2 + \frac{\beta}{4}e_2^4 + \frac{\gamma}{6}e_2^6 + \frac{\kappa}{2}|\nabla e_2|^2 \qquad (1)$$

where $A_2 = \alpha_T(T - T_c)$, $\beta < 0$, $\gamma > 0$ and $\kappa > 0$. Here $T_c$ is the low-stability limit of the high temperature phase.

As a consequence of the symmetry reduction, the nucleation and subsequent growth of the martensitic phase take place embedded within a host matrix of the austenitic phase. When the transformation goes on, in order to perserve coherency, the lattice is forced to reduce the average deformation along the phase boundary and hence the total energy. This process is called *self-accommodation* and gives rise to a microstructure of alternating variants of opposite strain.

A contribution from the non-OP strains ($e_1$ and $e_2$) is also included up to the harmonic term: $f_{\text{Non-OP}} = \frac{A_1}{2}e_1^2(\mathbf{r}) + \frac{A_3}{2}e_3^2(\mathbf{r})$. Notice that in 2D the three strain components $e_1$, $e_2$ and $e_3$ are not independent but they are linked by the so-called Saint-Vénant compatibility condition [8]. Moreover, the contributions of the non-OP strains $e_1$ and $e_3$ are energetically costly and therefore the domain structure should adopt the morphology that minimizes the total energy. These two conditions allow to express $f_{\text{Non-OP}}$ in terms only of $e_2$. This free energy shows, in real space, anisotropic long-range interactions whereas it becomes local in Fourier space:

$$f_{\text{Non-OP}} = \frac{A_3}{2(2\pi)^2}\frac{(k_x^2 - k_y^2)^2}{(\frac{A_3}{A_1})k^4 + 8(k_x k_y)^2}|e_2(\mathbf{k})|^2, \qquad (2)$$

where $e_2(\mathbf{k})$ is the Fourier transform of $e_2(\mathbf{r})$. We recall that $A_1$ and $A_3$ are the elastic constants $A_1 = C_{11} + C_{12}$ and $A_3 = 4C_{44}$ [9]. Indeed, cross-hatched correlations along the diagonal $k_x = \pm k_y$ are favored. The self-accommodation of martensite variants gives rise to a multidomain pattern called *twinning* where each of the variants is a *twin*.

Thus, the pure elastic energy is $f_{el} = f_{\rm L,G} + f_{\text{Non-OP}}$.

### B. Magnetic model

The spatial distribution of the local magnetization $\mathbf{M}(\mathbf{r})$ is used to describe the magnetic domain structure. This is a three dimensional continuous vectorial (spin) field. We define $\mathbf{m} \equiv \mathbf{M}/M_{\rm S} = (m_x, m_y, m_z)$ as the unit magnetization vector with $M_{\rm S}$ the saturation magnetization.

According to the micromagnetic theory [3],[10],[11], the magnetic energy in a solid magnetic body can be decomposed in the sum of the following terms:

$$f_{\rm m} = f_{\rm an} + f_{\rm exch} + f_{\rm ms} + f_{\rm ext} \qquad (3)$$

$f_{\rm an}$ is the magnetocrystalline anisotropy energy density, that is associated to the interaction of the magnetization with the anisotropic crystallographic undeformed lattice inducing a specific orientation of the spins. In a cubic system, $f_{\rm an}$ takes the form

$$f_{\rm an} = K_1(m_x^2 m_y^2 + m_x^2 m_z^2 + m_y^2 m_z^2) + K_2 m_x^2 m_y^2 m_z^2. \quad (4)$$

Here, $K_1$ and $K_2$ are the magnetocrystalline anisotropy constants. This potential will favor the diagonal directions (*easy axis of magnetization*).

The exchange energy density, $f_{\rm exch}$, accounts for variations of the magnetization through the solid:

$$f_{\rm exch} = A|\nabla \mathbf{m}|^2, \qquad (5)$$

where A is the exchange stiffness constant, that is positive (negative) for the ferromagnetic (antiferromagnetic) system. This term would correspond to the short-range dipole-dipole interaction of the Heisenberg model.

The magnetostatic energy density, $f_{\rm ms}$ accounts for the contribution coming from the long-range interactions between all local magnetic moments in the system via the demagnetization field $\mathbf{H}_d$, since from Maxwell equation $\nabla \cdot \mathbf{H} = -\nabla \cdot \mathbf{M}$.

$$f_{\rm ms} = -\frac{1}{2}\mu_0 M_s \mathbf{H}_d \cdot \mathbf{m}, \qquad (6)$$

where $\mu_0$ is the vacuum permeability.

Finally, $f_{\rm ext}$ is the interaction energy density between the magnetization and the external field.

$$f_{\rm ext} = -\frac{1}{2}\mu_0 M_s \mathbf{H}_{\rm ext} \cdot \mathbf{m} \qquad (7)$$

This energy orientates the spins along the direction of the field.

### C. Magnetoelastic coupling

The model takes into account the magnetoelastic coupling where the magnetization is coupled to the symmetry adapted strains [12]:

$$f_{me} = \frac{B_1}{\sqrt{2}}[(m_x^2 + m_y^2)e_1 + (m_x^2 - m_y^2)e_2] + B_2(m_x m_y)e_3, \quad (8)$$

where $B_1$ and $B_2$ are constants of magnetoelastic coupling.

Summarizing, the total free energy density is given by the summation,

$$f_T = f_{el} + f_m + f_{me}. \quad (9)$$

### D. Dynamics

The aim of the model is the study of stabilized states, which consist of magnetization and strain configurations that minimize the total energy (9). On the one hand, the stabilized strain configurations are reached by means of a pure relaxational dynamics defined by:

$$\frac{\partial e_2(\mathbf{r})}{\partial t} = -\frac{\delta F_T}{\delta e_2(\mathbf{r})} \quad (10)$$

On the other hand, the micromagnetic dynamical equation makes the magnetization evolve according to the Landau-Lifshitz-Gilbert (LLG) equation [11]:

$$(1+\alpha^2)\frac{\partial \mathbf{M}}{\partial t} = -\gamma_0 \mathbf{M}\times\mathbf{H}_{\text{eff}} - \frac{\gamma_0\alpha}{M_s}\mathbf{M}\times(\mathbf{M}\times\mathbf{H}_{\text{eff}}) \quad (11)$$

The first term in eq.(11) involves a precessional motion around the effective magnetic field $\mathbf{H}_{\text{eff}}$ and $\gamma_0$ is the gyromagnetic ratio. The second term is a damping term, that reduces the precession of spins around $\mathbf{H}_{\text{eff}}$ until reaching a static state of minimum energy. Here $\alpha$ is a dimensionless damping constant. The effective field can be calculated as $\mathbf{H}_{\text{eff}} = -\frac{1}{\mu_0}\frac{\partial F_T}{\partial \mathbf{M}}$. It is worth noting that the magnetoelastic couplig contributes to both dynamics, which gives rise to correlations between the strain and magnetization contributions.

## III. SIMULATION RESULTS

The numerical values for the model parameters are mainly those corresponding to $Fe_{70}Pd_{30}$ alloy (shown in table I). For the simulations, the model described above has been reformulated in reduced units [3], [11]. Discretization of the model and dynamics is carried out and implemented in a square mesh with periodic boundary conditions. The system is let evolve until reaching a stabilized configuration in both strain and magnetization degrees of freedom.

| Symbol | Value (S.I units) | Symbol | Value (S.I units) |
|---|---|---|---|
| $\alpha_T$ | $2.4\cdot10^{8}$ N/(m$^2$K) | $\Lambda$ | $4.55\cdot10^{-10}$ m |
| $A_3$ | $28\cdot10^{10}$ N/m$^2$ | $M_s$ | $1.08\cdot10^{6}$ A/m |
| $A_1$ | $14\cdot10^{10}$ N/m$^2$ | $K_1$ | $-5.2\cdot10^{2}$ N/m$^2$ |
| $T_c$ | 257 | $K_2$ | $-6.6\cdot10^{4}$ N/m$^2$ |
| $\beta$ | $1.7\cdot10^{13}$ N/m$^2$ | $B_1$ | $-1.85\cdot10^{8}$ N/m$^2$ |
| $\gamma$ | $3\cdot10^{16}$ N/m$^2$ | $B_2$ | $-6.72\cdot10^{7}$ N/m$^2$ |
| $\kappa$ | $3.5306\cdot10^{-9}$ N | $A$ | $10^{-12}-10^{-13}$ N/m$^2$ |

TABLE I. Symbols and values in S.I of the parameters of the model. Extracted from Ref [3].

### A. Preliminary results

In this section, we start studying the pure elastic model, without the magnetic contribution. Figure 3 shows the MT induced either by temperature ($a$) or by an external stress field ($b$), simulated in a 256x256 cell.

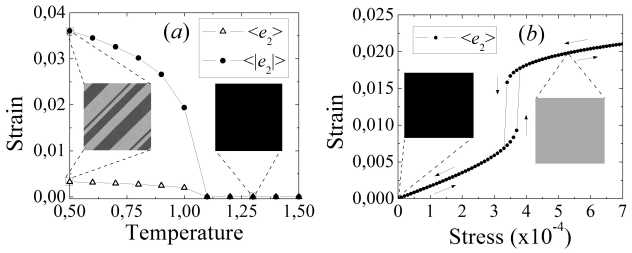


FIG. 3. Martensitic transformation: ($a$) The strain-temperature curve at zero applied stress field. ($b$) The strain-stress curve at constant temperature ($T > T_c$).

In panel ($a$) we can observe that below $T_c$, the system exhibits non-zero values of $\langle|e_2|\rangle$ with a multidomain microstructure, that corresponds to the martensitic phase with twinning pattern. Above $T_c$, the stable phase is austenite so that the local strain is zero. In panel ($b$), we can see the MT induced by external stress field. Initially, we start from austenitic phase and, progressively, we increase the external stress field. During the load of the stress, the system first undergoes simple elastic deformation. Then, for certain value of the stress field, a sharp increase in the average strain is observed due to the stress-induced transition giving rise to a monovariant martensitic phase. Unloading the stress field, the system transforms back to the austenitic phase so that the unit cell recovers its initial shape. This effect corresponds to the superelastic behavior and, during the load-unload process, it can gives rise to hysteresis effects.

Figure 4 shows the ($\sigma$-$e_2$-$T$) curve corresponding to the shape memory effect (SME). The snapshots show representative configurations at a given value of ($\sigma$,$e_2$,$T$). They have been labeled to make clear the order of the sequence. We can identify different processes. Focusing on the ($\sigma$-$e_2$) curve at $T = 0.52$ ($< T_c$), pseudoplastic behavior is observed: (i)-(iii) correspond to increasing the stress, starting from twinned martensite (with an average strain near zero), until a monovariant martensitic

phase is obtained due to the reorientation of the twins. (iii)-(iv) correspond to unload of the stress and we can see that the system maintains the single domain configuration. Finally, (iv)-(vi) show the $(e_2 - T)$ curve where the system is heated at zero external stress field until it transforms to the austenitic phase, where the initial macroscopic shape is recovered.

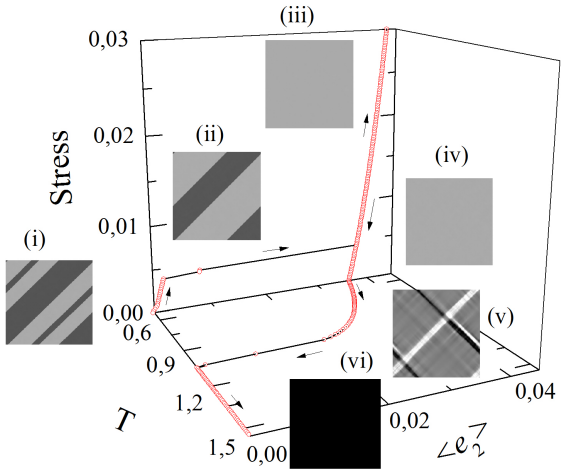


FIG. 4. Shape memory effect (SME). Snapshots show the evolution of the microestructure in different points of the curve.

### B. Magnetoelastic results

In this section we present the simulation results of the full magnetoelastic model. In Figure 5$(a)$ we show the stable magnetic configuration obtained on a 512x512 system at $T = 0.5$ and compare it with the experimental observation in the case of martensite with magnetization domains $(b)$. One can observe multidomain magnetic mi-

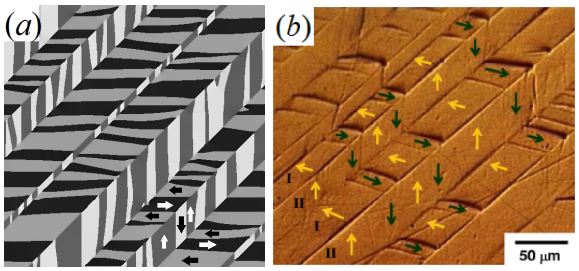


FIG. 5. Comparison between a stable magnetic configuration obtained by numerical simulation $(a)$ and the experimental martensite with magnetization domains $(b)$, extracted from [13].

crostrucures. Here, arrows represent the direction of the magnetization in a given domain in the plane X-Y. The elastic twins induce the magnetization to align to specific directions (horizontal or vertical) according to the particular variant due to the magnetoelastic coupling. Therefore, the change in the magnetization vector from one twin to another occurs across 90° domain walls that coincide with the twin boundaries. Moreover, within each twin, magnetic stripes separated by 180° type domain walls are formed. Such a magnetic arrangement allows the minimization of the overall magnetostatic energy.

Figure 6 shows the dependence of both strain (upper panels) and magnetization (lower panels) on temperature at zero magnetic field $h = 0$ $[(a)$-$(b)]$ and at different values of the applied $h$ $[(c)$-$(d)]$. We note that $(a)$ ex-

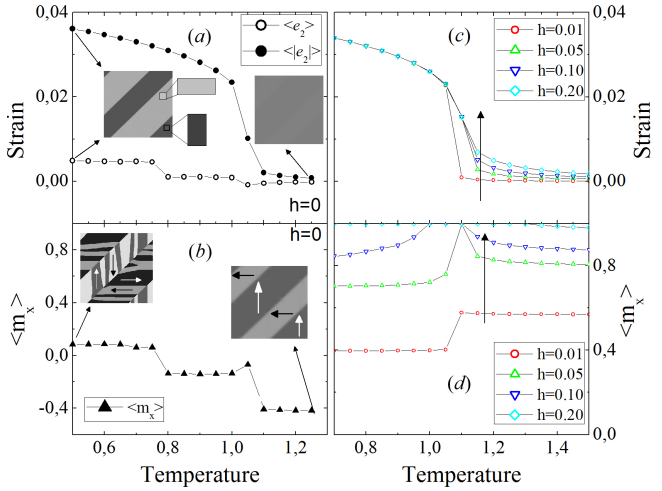


FIG. 6. Strain-temperature and magnetization-temperature curves: $(a)$-$(b)$ at zero applied external field, $(c)$-$(d)$ for different values of applied external field.

hibits a similar behavior to Fig. 3$(a)$, and the martensitic transformation is observed. The Fig. 6$(b)$ is the corresponding $\langle m_x \rangle$ dependence with the temperature. The multidomain magnetic microstructure below $T_c$ is again observed, where the different elastic twins determine the preferred magnetization direction. We can observe at high temperature that the austenite phase exhibits a small strain and this is also reflected in the magnetization direction due to the strong magnetoelastic coupling. This behavior has been observed experimentaly in [14] When applying an external magnetic field , we can see in panel $(c)$ that the average strain values in austenitic phase increases for larger values of applied magnetic field. This reflects the existence of a cross-response between the strain and the applied magnetic field. On the other hand, in a heating process, an increase of $\langle m_x \rangle$ ($h$ field direction) is observed in Fig. 6$(d)$ between the martensitic phase and austenitic phase. This is in qualitative good agreement with experimental observations [15].

The magnetic shape memory effect (MSME) is reproduced in Fig. 7. Initially, we start from twinned martensite at $T = 0.5$ and zero applied magnetic field, where the magnetic domains are oriented depending of the elastic twin, according to the described for the Fig. 5. In this point, snapshot (i), the system exhibits $\langle e_2 \rangle \simeq 0$ and $\langle m_x \rangle = \langle m_y \rangle \simeq 0$. The increase of the magnetic field, (i)-(iv), causes the reorientation of the magnetization in

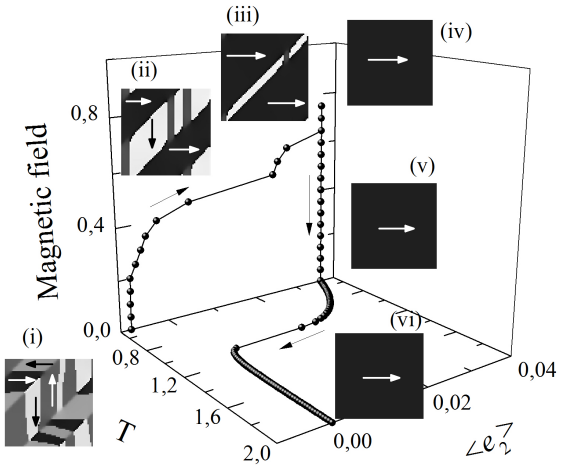


FIG. 7. Magnetic Shape Memory Effect (MSME). Snapshots of 64x64 simulation cells show the evolution of the microstructure of magnetic domains in representative points of the curve.

such a way that it leads to the growth of the elastic variant coupled to the magnetization component favored by the external field. The system exhibits nonzero macroscopic strain when the magnetic saturation is reached. Progressively, we decrease the magnetic field until it is zero and we can observe that both strain and magnetization are kept practically constant (snapshot (v)). Finally, in the $(e_2 - T)$ curve (snapshots (v)-(vi)) the system is heated at zero applied magnetic field until it reaches the austenitic phase, where the initial macroscopic shape is recovered. The austentitic phase has a residual deformation which is sufficient to cause that the system remains magnetically saturated. This behavior has been observed in many FSMAs [4], [5], [16], [17].

## IV. CONCLUSIONS

The results presented in this work show that the pure elastic model is able to reproduce the martensitic phase with twinned pattern and the martensitic transition induced both by temperature and by the external stress. The shape memory effect and the superelasticity is also obtained. The full magnetoelastic model is able to reproduce the typical magnetic microstructure at low temperature. This microstructure consists of magnetic stripes within martensitic twins. We can see the martensitic transformation induced by temperature at different values of applied magnetic field and the MSME where we could observe the elastic and magnetic configurations and correlations between them due to the magnetoelastic coupling. In light of preliminar results not shown here, the model shows capabilities to reproduce other experimental observations such as magnetic superelasticity.

## ACKNOWLEDGMENTS

First of all, I would like to thank my advisor Prof. Teresa Castán for her very valuable scientific and personal support. I would also like to thank Pol Lloveras for his great help, encouragement and availability along the year. All this would not have been possible without the support and patience of the people close to me.

[1] V. K. Wadhawan, *Introduction to ferroic materials* (Gordon and Breach Science Publishers, Amsterdam, 2000).
[2] N. A. Spaldin *et al.* "Multiferroics: Past, present, and future", Physics Today **63**, 38 (2010).
[3] P. Lloveras, "Interplay between anisotropy and disorder in ferroelastics: Structures and thermodynamics". Ph.D. Thesis, UB, Barcelona, 2010.
[4] H.E. Karaca *et al.* "Magnetic field and stress induced martensite reorientation in NiMnGa ferromagnetic shape memory alloy single crystals", Acta Mater. **54**, 233-245 (2006).
[5] O. Heczko, "Magnetic shape memory effect and magnetization reversal", J. Magn. Magn. Mater. **290-291**, 787-794 (2004).
[6] J. M. Sancho, *Física Estadística: Sistemas en Interacción*, (Edicions UB, España 2011).
[7] L.D. Landau and E. M. Lifshitz, *Theory of Elasticity* (Pergamon Press, Oxford, 1986).
[8] T. Lookman *et al.* "Ferroelastics dynamics and strain compatibility", Phys. Rev. B **67**, 024114 (2003).
[9] S. Kartha *et al.* "Disorder-driven pretransitional tweed pattern in martensitic transformation", Phys. Rev. B **52**, 803-822 (1995).
[10] A. Morrish, *The physical principles of magnetism* (Wiley, New York, USA, 1995).
[11] J. Zhang and L. Chen, "Phase-field microelasticity theory and micromagnetic simulations of domain structures in giant magnetostrictive materials", Acta Mater. **53**, 2845 (2005).
[12] C. Kittel, "Physical Theory of Ferromagnetic Domain", Rev. Mod. Phys. **21**, 541-583 (1949).
[13] J. N. Armstrong *et al.* "Role of magnetostatic interactions in micromagnetic structure of multiferroics", J. Appl. Phys. **103**, 0239051-5 (2008).
[14] M. R. Sullivan and H. D. Chopra, "Temperature-and field- dependent evolution of micromagnetic structure in ferromagnetic shape-memory alloys", Phys. Rev. B **70**, 094427 (2004).
[15] A. Planes *et al.* "Magnetocaloric effect and its relation to shape-memoy properties in ferromagnetic Heusler alloys", J. Phys.: Condens. Matter **21** 233201 (2009).
[16] Y. Ge *et al.* "Various magnetic domain structures in a NiMnGa martensite exhibiting magnetic shape memory effect", J. Appl. Phys. **96**, 2159 (2004).
[17] Y. Ge *et al.* "Magnetic domain evolution with applied field in a NiMnGa magnetic shape memory alloy", Phys. Rev. B **54**, 2155-2160 (2006).